A Brief Overview of Citrine's Data and Informatics Platform

Bryce Meredig
Citrine Informatics

CHiMaD Meeting
2 May 2016

The Citrine Platform Architecture

Shinier Paint | Tougher Phones | Lighter Vehicles | Greener Suppliers

Machine Learning and Apps

Citrine and third parties can build powerful analytics for physical product companies

World's Largest Physical Data Platform

Citrine is consolidating vast stores of physical knowledge

Data Extraction from Documents

Citrine's extraction engine ingests quantitative data from research papers, patents, data sheets

Data Streaming from Users

Customers and a growing network of government and university labs push data to our platform

The Industrial Materials Design Problem

CUSTOMER PROJECT: FORMULATION DEVELOPMENT

90
possible physical inputs

35
product features need optimization

10^{89}
combinations represent overwhelming search space

Global Leaders Choose Citrine

Aerospace

Boeing, HRL Laboratories

Materials

Fortune 200 materials co.

Defense

DARPA

Electronics

Panasonic

Automotive

Hyundai

Alloys

Alcoa

Large-Scale Data and AI for All Materials

Thermoelectrics

25k precomputed & 1.5k user-requested materials
Users at NASA, LBNL, MIT

Aluminum Alloys

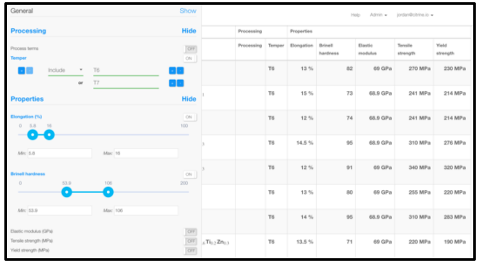

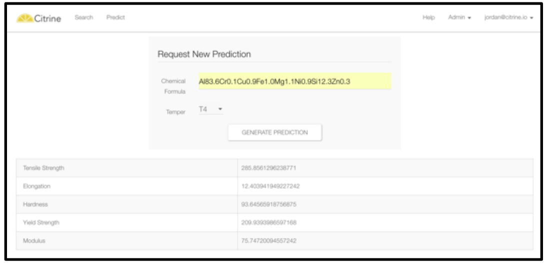

World's largest ML-ready Al alloy database
AI-based models of properties

Steel

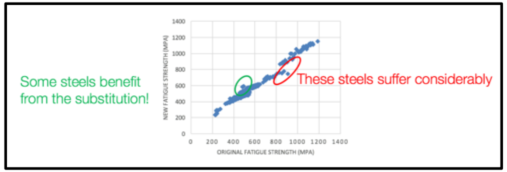

Web-based models for real-time steel design

Plus customer use cases: coatings, energy materials, epitaxy, next-generation aerospace alloys, …

Missing Link in the Materials Genome

Real-time, easy-to-use, web-based data infrastructure and predictive tools

A metallurgist can go to
citrination.com/alloys/predict
and input composition and temper

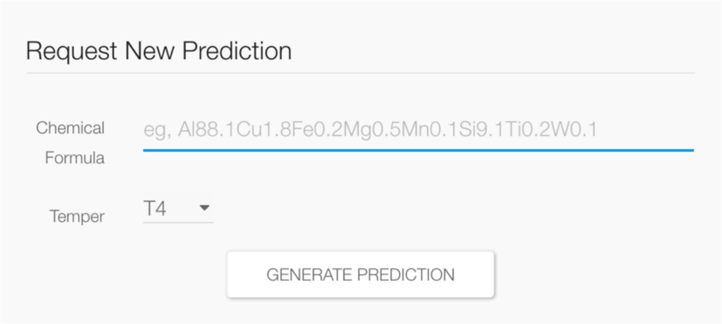

In a few seconds, user receives AI output
No programming, learning curve, or waiting

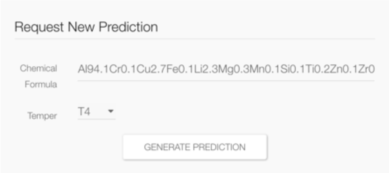

Tensile Strength	422.13955479644636
Elongation	13.072276636619629
Hardness	115.24441342594316
Yield Strength	316.5495388684673
Modulus	76.0

AI-Based Models Are Very Accurate

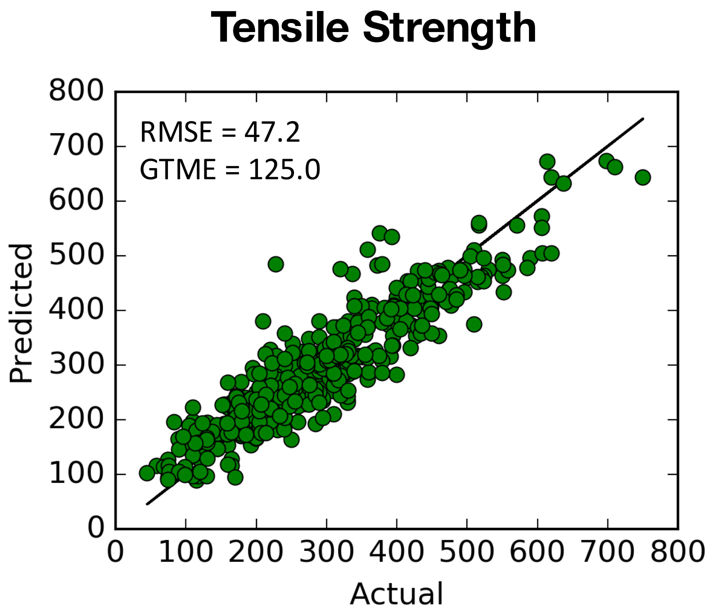

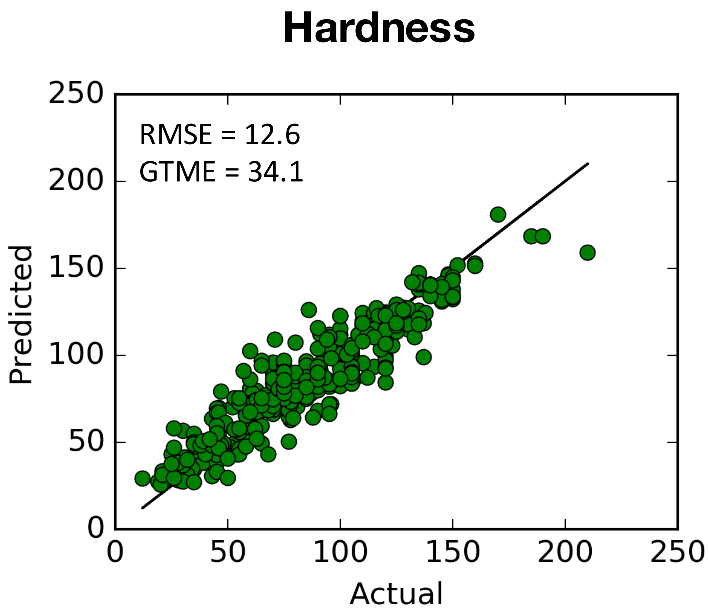

One organization that has made significant progress in establishing a centralized data resource for materials scientists is **Citrine Informatics**, a company that specializes in applying data mining to materials discovery and optimization.

—Ceder, Jain, Persson

APL Materials

http://dx.doi.org/10.1063/1.4944683

Statistics on Citrination.com

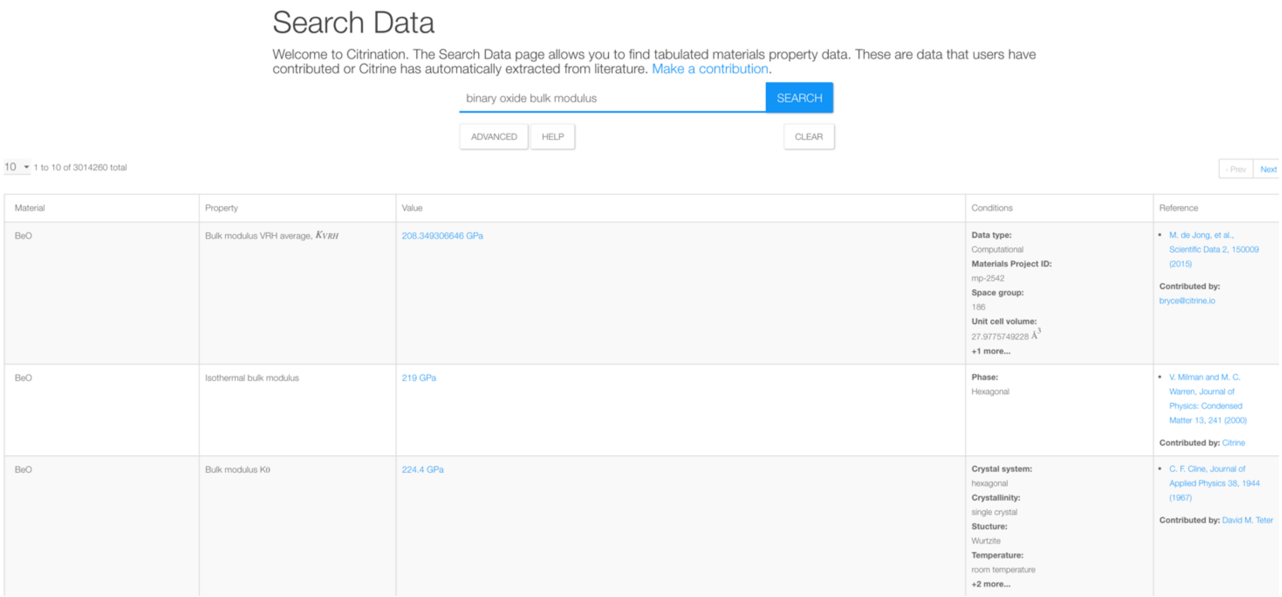

3.1m free data records

Users from almost 2k institutions worldwide

Data Extraction: Text

Kinetics of premartensite to martensite transition and its implications on the origin of modulation in Ni_2MnGa ferromagnetic shape memory alloy

Sanjay Singh[1], J. Bednarcik[2], S. R. Barman[3], C. Felser[1], and Dhananjai Pandey[4]

[1] Max Planck Institute for Chemical Physics of Solids, Nöthnitzer Strasse 40, D-01187 Dresden, Germany

[2]Photon Sciences, FS-PE, Deutsches Elektronen Synchrotron (DESY), 22607 Hamburg, Germany

[3]UGC-DAE Consortium for Scientific Research, Khandwa Road, Indore, 452001, India.

[4]School of Materials Science and Technology, Indian Institute of Technology(Banaras Hindu University) , Varanasi-221005, India.

Abstract

We present here results of temperature dependent high resolution synchrotron x-ray powder diffraction study of sequence of phase transitions in Ni_2MnGa. Our results show that the incommensurate martensite phase results from the incommensurate premartensite phase, and not from the austenite phase assumed in the adaptive phase model. The premartensite transforms to the martensite phase through a first order phase transition with coexistence of the two phases in a broad temperature interval (~40K), discontinuous change in the unit cell volume as also in the modulation wave vector across the transition temperature and considerable thermal hysteresis in the characteristic transition temperatures. The temperature variation of the modulation wave vector q shows smooth analytic behavior with no evidence for any devilish plateau corresponding

confirms the cubic structure in the Fm-3m space group (see Fig 3a). The cell parameter (a= 5.82445(1) Å) obtained by us is in good agreement with those reported by earlier workers. [7, 11]

cell parameter a = MATERIALS PROPERTY
5.82445(1) = NUMERICAL VALUE
angstrom = UNITS

Extraction: Images & Tables

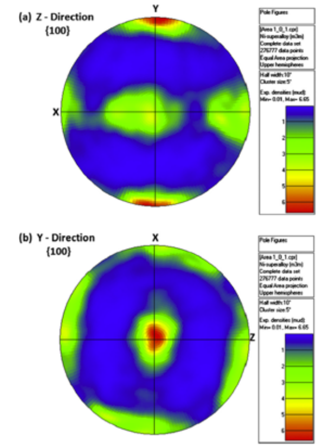

Fig. 20. {100} pole figures for the simple scan pattern CM247LC with respect to the (a) *Z* (build) direction and (b) *Y* (laser scan) direction.

Image: **0.84**
Plot: 0.06
Table: 0.10

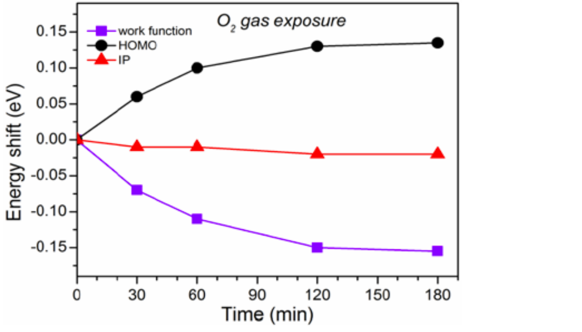

Fig. S2: Work function, HOMO and IP plots of PCBM film as function of *in situ* O_2 exposure time. WF shows a down shift and HOMO has an upward shift, but IP keeps constant.

Image: 0.02
Plot: **0.94**
Table: 0.04

p_c	Method	Reference
Nishimori point in the $\pm J$ model		
0.111 ± 0.002	Transfer matrix	[30]
0.114 ± 0.003	Series expansion	[17]
0.1128 ± 0.0008	Non-equilibrium	[31]
0.1095 ± 0.0005	Transfer matrix	[18]
0.1094 ± 0.0002	Transfer matrix	[15]
0.1093 ± 0.0002	Fermionic transfer matrix	[19]
0.110028	Duality	[21]
≤ 0.178203	Rigorous upper bound	[32]
$T = 0$ critical point in the $\pm J$ model		
~ 0.099	Series expansion	[22]
0.105 ± 0.01	Matching algorithm	[23]
$0.095 < p_c < 0.108$	Matching algorithm	[24]
0.104 ± 0.001 0.106 ± 0.002	Exact ground states	[25]
0.115	Ground state enumeration	[27]
0.1031 ± 0.0001	Exact ground states	[12]
0.103 ± 0.001	Exact ground states	[28]

Image: 0.02
Plot: 0.00
Table: **0.98**

Extraction: Images & Tables

Image containing data

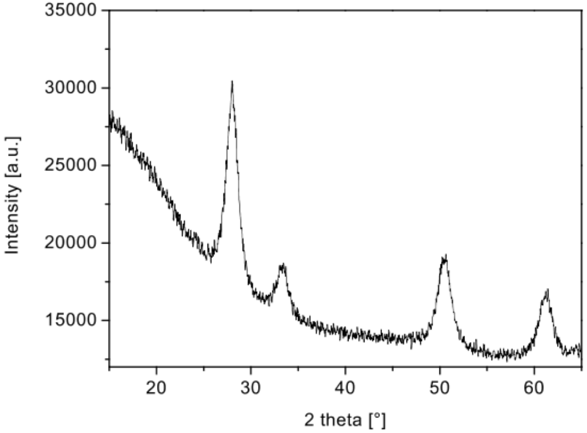

machine vision

Underlying x,y data
(actual extraction shown)

2theta[°]	Intensity[a.u.]
28.113381	32034.0536
28.113381	31965.0781
28.113381	31896.1026
28.113381	31827.1271
28.113381	31758.1516
28.113381	31689.1762
28.113381	31620.2007
28.0006952	31551.2252
28.113381	31551.2252
28.0006952	31482.2497
28.113381	31482.2497
28.0006952	31413.2742
28.113381	31413.2742
28.0006952	31344.2987
28.113381	31344.2987
28.0006952	31275.3232
28.113381	31275.3232
28.0006952	31206.3477
28.0006952	31137.3722
28.2260668	31137.3722
28.0006952	31068.3967
28.2260668	31068.3967
28.0006952	30999.4212
28.2260668	30999.4212
28.0006952	30930.4457
28.2260668	30930.4457

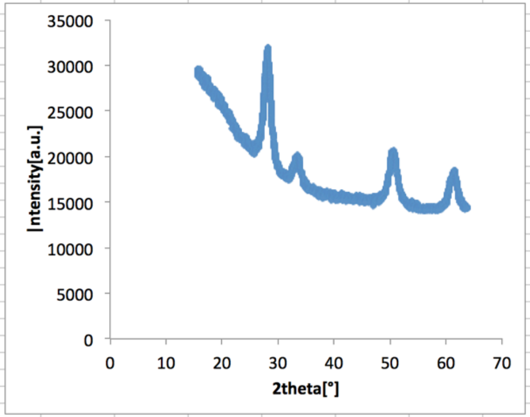

Extraction in Production Today

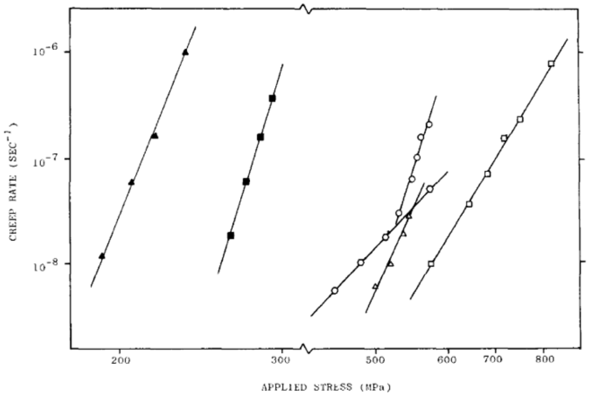

Fig. 1. The creep rates as a function of applied stress at 760 °C: ▲, MA 754; ■, MA 753; ○, MA 6000E; △, Nimonic 115; □, Mar M200; ⬭, Udimet 700.

Material	Property	Value	Conditions	Reference	Actions
MA 754	Creep rate	1.1e-07 to 9.7e-06 s^{-1}	**Applied stress:** 191.45 to 235.71 MPa **Temperature:** 760 °C	• The Role of the Alloy Matrix in the Creep Behaviour of Particle-strengthened Alloys; Materials Sciences and Engineering 44 (1980) 165-172 **Contributed by:** Jo	
MA 753	Creep rate	1.8e-07 to 3.5e-06 s^{-1}	**Applied stress:** 264.07 to 292.75 MPa **Temperature:** 760 °C	• The Role of the Alloy Matrix in the Creep Behaviour of Particle-strengthened Alloys; Materials Sciences and Engineering 44 (1980) 165-172 **Contributed by:** Jo	

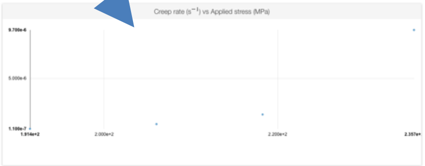

Value & Conditions

Material: **MA 754** Measurement: **Creep rate**

1.1e-07 to 9.7e-06 s^{-1}

Applied stress

191.45 to 235.71 MPa

Temperature

760 °C

Data Partnerships

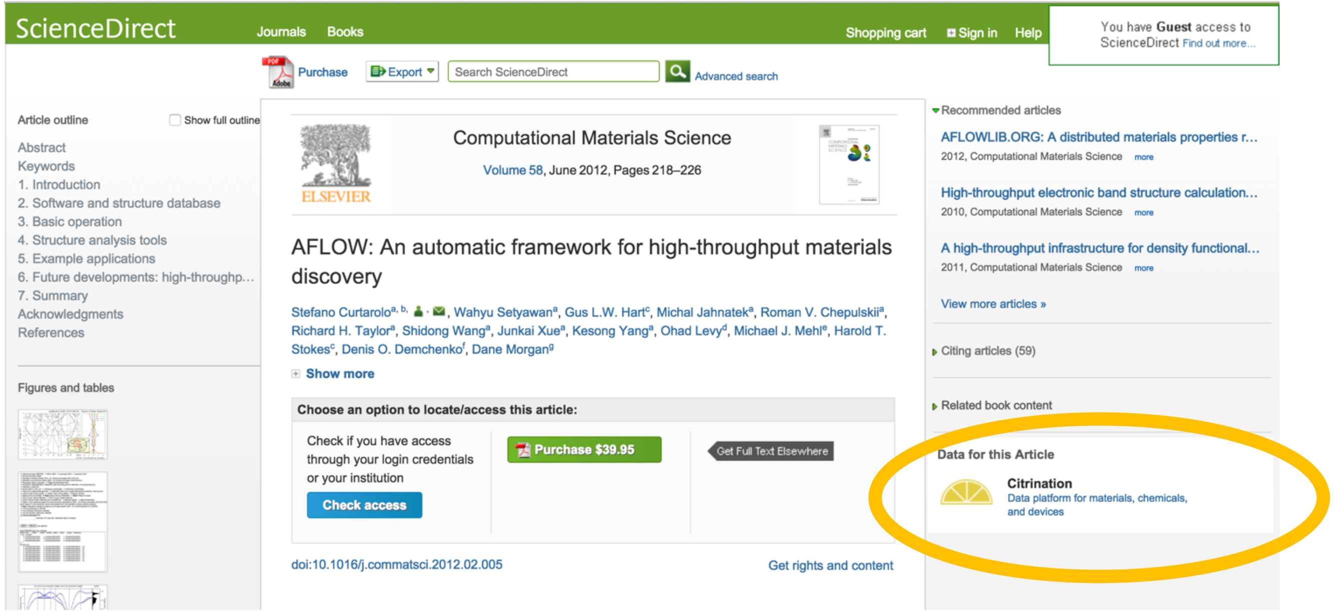

Data Partnerships

Energy & Environmental Science

PAPER

View Article Online
View Journal

CrossMark
click for updates

Cite this: DOI: 10.1039/c5ee03488d

Development of solar fuels photoanodes through combinatorial integration of Ni–La–Co–Ce oxide catalysts on $BiVO_4$†

D. Guevarra,‡[a] A. Shinde,‡[a] S. K. Suram,[a] I. D. Sharp,[bc] F. M. Toma,*[bc] J. A. Haber*[a] and J. M. Gregoire*[a]

Acknowledgements

This material is based upon work performed by the Joint Center for Artificial Photosynthesis, a DOE Energy Innovation Hub, supported through the Office of Science of the U.S. Department of Energy (Award No. DE-SC0004993). The authors thank Citrine Informatics (www.citrine.io) for data hosting. The raw potentiostat and spectrometer data for the anodic sweep of the CV for each photoanode are available at links.citrination.com/ni-la-co-ce.